Experiments with a laser cooled cloud of atoms

Vasant Natarajan, Ayan Banerjee and Umakant Rapol

Department of Physics, Indian Institute of Science, Bangalore 560 012, India

We discuss two experiments that can be performed using a cloud of laser-cooled and trapped atoms, namely Bose–Einstein condensation (BEC) and search for a permanent Electric Dipole Moment (EDM). BEC can be observed in Rb atoms in a magnetic trap by using forced evaporative cooling to continuously lower the temperature below the condensation limit. The cloud is cooled by preferentially ejecting the hottest atoms from a magnetic trap. The magnetic trap is loaded with laser-cooled atoms from a magneto-optic trap. The EDM experiment can be performed with a laser-cooled cloud of Yb atoms. The atoms are spin polarized and the precession of the spin is measured in the presence of a strong electric field applied perpendicular to the spin direction. The use of laser-cooled atoms should greatly enhance the sensitivity of the experiment.

OVER the last two decades, there has been tremendous excitement in the field of atomic physics with the development of techniques to laser cool and trap clouds of neutral atoms. In recognition of these efforts, the Nobel Prize in Physics for 1997 was jointly awarded to Steven Chu of Stanford University (USA), Claude Cohen-Tannoudji of Ecole Normale Superieure (France), and Williams Phillips of NIST at Gaithersburg (USA). The techniques they have helped in developing may have a wide impact ranging from fundamental measurements in physics to nanoscale technology of the future.

The advent of inexpensive tunable diode lasers has put these experiments well within the reach of researchers across the world operating on low budgets. Many of the laser cooling experiments have been performed on alkali atoms such as Li, Rb and Cs, which have transitions in the 670–850 nm range that are easily accessible with commercial semiconductor diode lasers. The technology to get stable single-frequency operation from laser diodes is now simple enough for such experiments to be set up in India. For example, in Figure 1 we show the saturated absorption spectra from Rb atoms in a vapour cell obtained with a grating stabilized diode laser in our laboratory. The design for the stabilization is similar to that given in ref. 1.

The other papers in this special issue of *Current Science* present details of laser diode stabilization and the techniques for cooling and trapping of alkali atoms in a vacuum chamber. The techniques described in those papers can be used to achieve what is generally the starting point of most laser cooling experiments, namely the magneto-optic trap (MOT). In this paper, we will concentrate on the different kinds of experiments that can be performed once a cold cloud of atoms is achieved.

Bose–Einstein condensation

The most fascinating advancement using the techniques of laser cooling and trapping has been the observation of Bose–Einstein condensation (BEC) in clouds of alkali atoms[2,3]. BEC is a phase transition that occurs purely due to the quantum indistinguishability of particles. At a sufficiently low but finite temperature, a macroscopic fraction of particles occupies the ground state of the system. In the case of trapped atoms, this state is the quantum ground state of the trap. The experiment requires three main steps, and we will take Rb as our candidate species since this is the easiest system in which to observe BEC.

To begin with, the MOT used for BEC experiments should preferably be a double MOT of the kind shown schematically in Figure 2. The double MOT for Rb trapping is usually a UHV glass chamber which has two
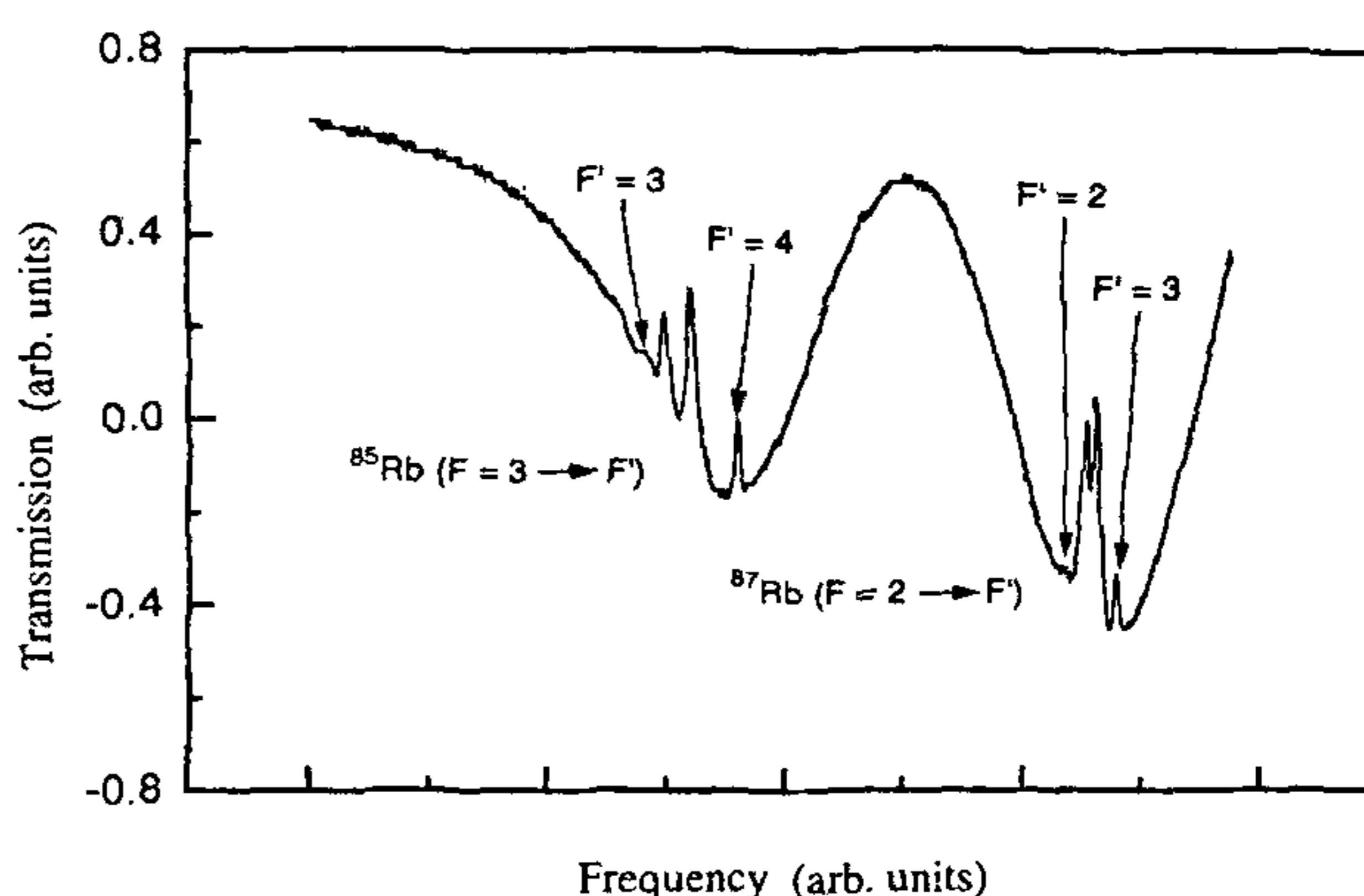

Figure 1. Saturated absorption spectra from Rb atoms. The spectra were obtained using a grating stabilized diode laser[1] and a Rb vapour cell at room temperature. The broad dips correspond to the Doppler broadened absorption (about 500 MHz wide) of the weak probe beam, while the sharp peaks appear when the transition is saturated by a strong counter-propagating beam.
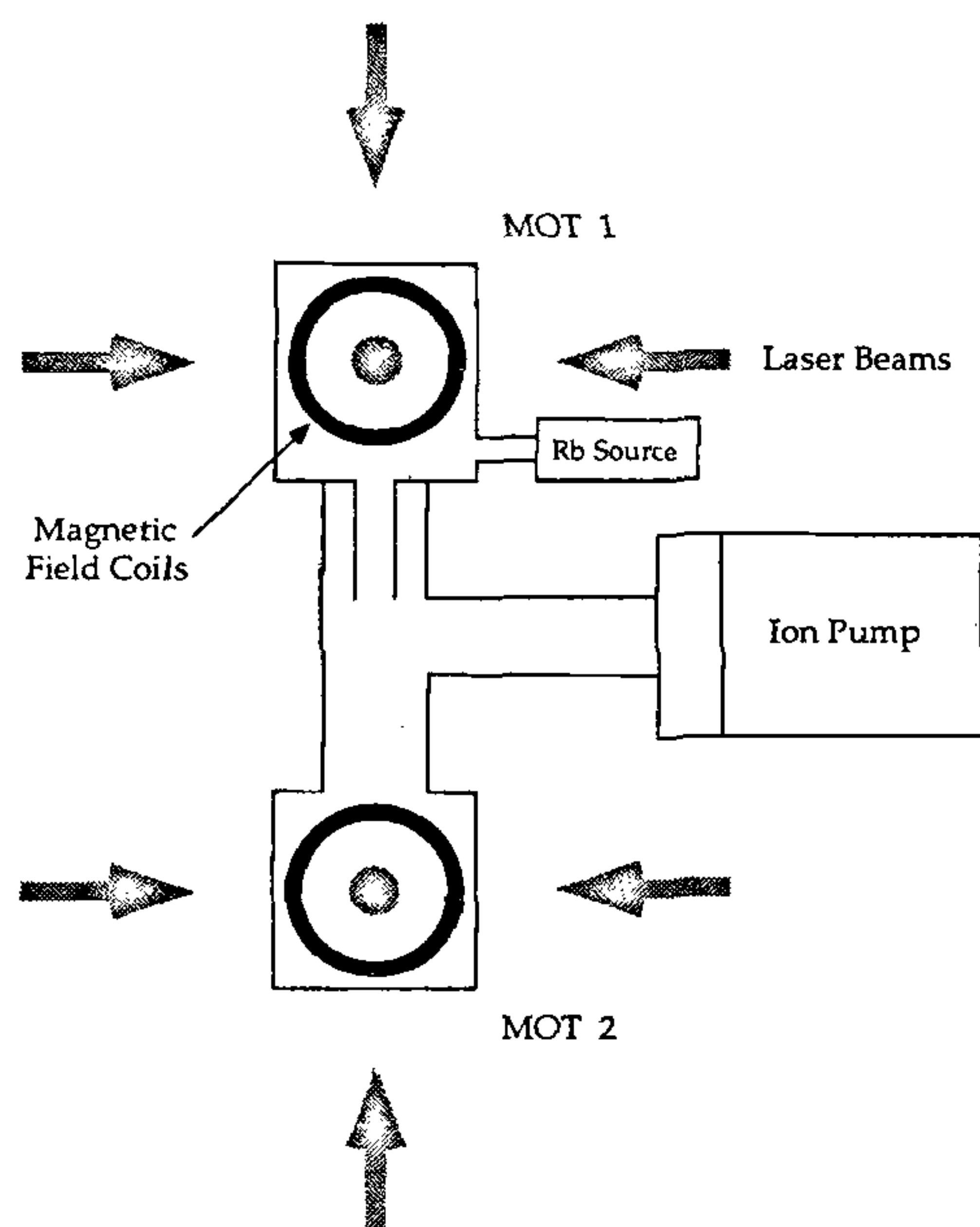
Figure 2. Schematic for a double MOT for Rb atoms. The upper trap has a relatively poor vacuum and is used for capturing atoms from a background vapour. It has two circular coils for producing the quadrupole magnetic field. The lower trap has a better vacuum and is used for observing BEC. It has four additional current carrying rods (not shown) to produce a magnetic trap with a non-zero field at the trap center (Ioffe-Pritchard trap). Each trap has six intersecting circularly-polarized laser beams, four beams as shown and two beams perpendicular to the plane of the figure.

separate trapping regions, one close to the Rb source where the vacuum is relatively poor (of order 10^{-8} torr) and which is used to capture atoms from a vapour, and a second region of much better vacuum (of order 10^{-10} torr) where the trap lifetimes are higher owing to the lower background pressure. The different vacuum levels in the two regions can be maintained by a scheme of differential pumping as shown in the figure. In addition, a Ti-sublimation pump may be used in the high vacuum region to increase the local pumping speed.

For the experiment, Rb atoms are initially loaded into the first trap from a background vapour using a combination of Doppler cooling and polarization-gradient cooling. Once a high enough density of atoms (about $10^{11}/cm^3$) has been achieved, the cloud is transferred to the second MOT region using a moving molasses configuration, where the frequency of the vertical laser beams is adjusted so that they cool the atoms in a frame of reference moving downwards with respect to the laboratory frame[4]. For example, if the detuning of the molasses beam pointing down in Figure 2 is changed from –20 MHz to 80 MHz and the detuning of the beam pointing up is changed from –20 MHz to –120 MHz,

then the atoms will be cooled in a reference frame moving downwards at a velocity that produces a Doppler shift of 100 MHz, or 78 m/s for Rb atoms. The frequencies are returned to their original values once the atoms arrive at the second trapping region. Controlled and variable frequency shifts of this kind can easily be produced using acousto-optic (AO) shifters driven by appropriate rf drivers.

The second step, after the atoms are loaded in the high vacuum MOT, is to turn off the MOT laser beams, spin polarize the atoms, and convert the MOT into a pure magnetic trap. Spin polarization is achieved using optical pumping into the appropriate magnetic sublevel with a pulse of circularly polarized light[2]. The quantization axis is set by the direction of the optical pumping beam. Once the atoms all have their spins pointing in the right direction, the current through the MOT coils is increased to increase the quadrupole magnetic field. Atoms are trapped in such a magnetic trap by the interaction of their magnetic moment with the field (given by $-\mu \cdot B$). However, a pure spherical quadrupole field, which has a zero-field point at the trap minimum, is not useful for BEC experiments. This is because the trapped and untrapped states are degenerate at the zero-field point and there is a possibility of a non-adiabatic spin flip (Majorana flip) as atoms pass through this point. The coldest atoms which are near the trap minimum are therefore steadily lost from the trap.

One solution to this problem is to use the Ioffe-Pritchard field configuration[5,6] which has a non-zero bias field at its minimum. Such a field can be produced by using 4 current carrying bars in addition to the MOT coils as shown in Figure 3. The current through the coils is determined by numerically solving Maxwell's equations for the chosen coil sizes and desired values for the bias field and field curvature near the origin. Typically, about 50–100 A of current will be needed, so some form of active cooling for the coils is essential. In Figure 3, we show the results of a numerical calculation for coils of diameter 3 cm placed 4.5 cm apart. The four straight wires lie symmetrically on a circle of radius 1 cm. As can be seen from the profile of the magnetic field along the z-axis, the trap is fairly parabolic and has a minimum field of about 15 G.

The final step on the road to BEC is forced evaporative cooling in the magnetic trap. For this, the hottest atoms are forced into an untrapped state (i.e. their spins are flipped) by driving the magnetic dipole spin flip transition at a chosen rf frequency[7]. The value of the rf frequency determines the value of the magnetic field where the atoms are resonantly driven into the untrapped state. Since the field increases as one moves away from trap center, only hot atoms (having a velocity larger than a critical value) will reach the point where their spins are flipped, and only these hot atoms will be ejected from the trap. The remaining atoms then thermalize to
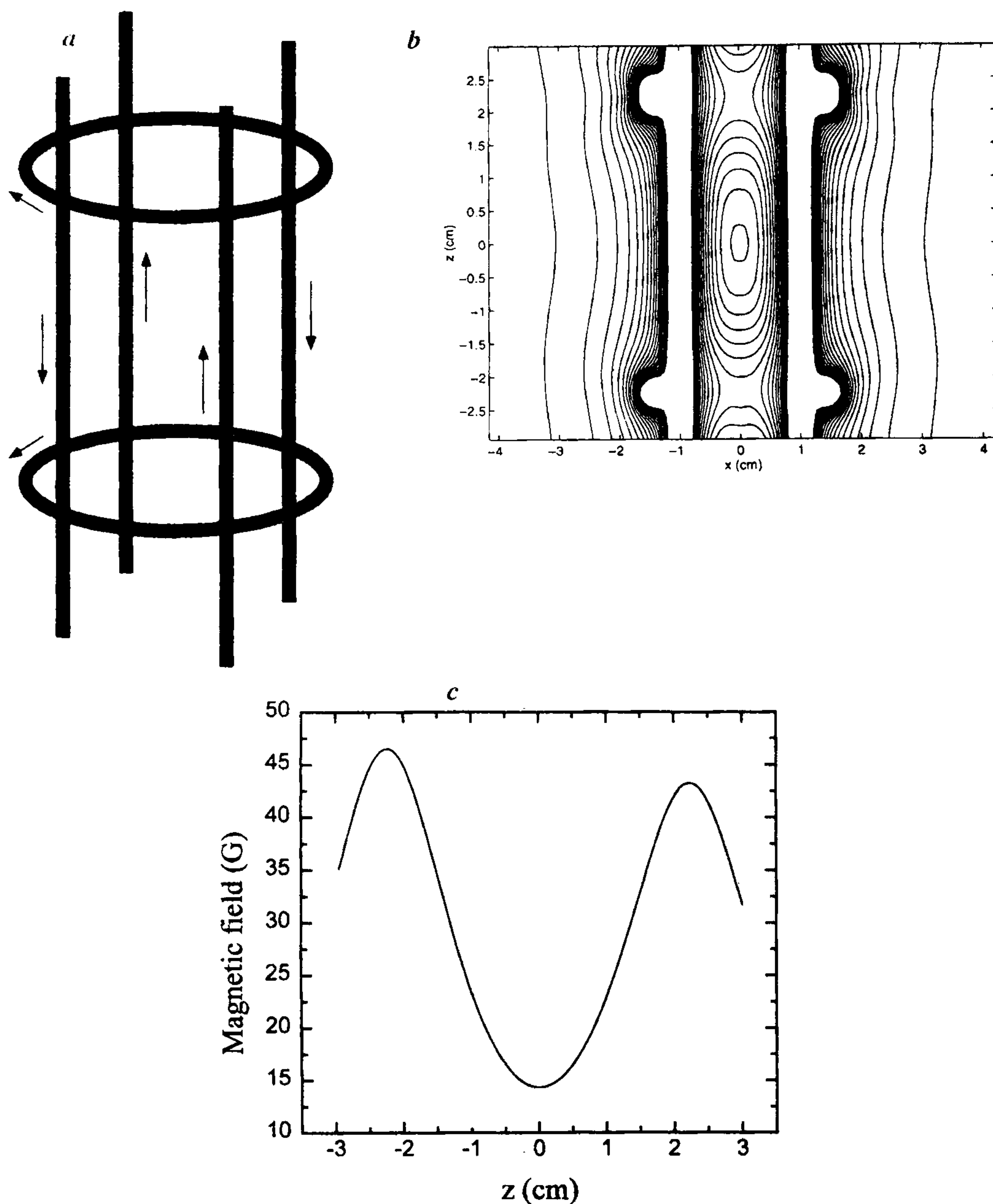
Figure 3. Magnetic field profiles in a Ioffe-Pritchard trap. The field is calculated by numerically solving Maxwell's equations for the coil configuration shown in (*a*). The coils have a diameter of 3 cm and a separation of 4.5 cm. The four current carrying rods lie symmetrically on a circle of radius 1 cm. Shown in (*b*) are the field contours (in intervals of 5 G) for a vertical plane through the middle of the trap and passing through two diagonal rods. The field along the *z*-axis, plotted in (*c*), has a parabolic shape and a non-zero minimum of 14.3 G.

an overall lower temperature. Under the right conditions of large elastic collision rate for the atoms and low trap losses due to background gas collisions, this process of evaporative cooling can be carried out indefinitely until BEC is achieved. The rf coils used for driving the spin flip transition are similar to coils used in nuclear magnetic resonance (NMR) experiments.

Two important points are to be noted. The high vacuum MOT has a region near the center where the repumping laser light is blocked out[8]. This increases the

density in the trap by shelving the coldest atoms into the 'wrong' hyperfine state where they stop interacting with the laser light and hence do not get heated. Further, once the atoms are loaded into the magnetic trap, the field gradients are increased adiabatically to compress the cloud. This increases the elastic collision rate which is important for efficient evaporative cooling[9].

After evaporative cooling, the cold cloud is imaged by near-resonant absorption imaging using a weak probe laser. The cloud is allowed to expand ballistically for a short time (of order few ms) with the trapping fields turned off so that the image displays the initial velocity distribution of the trapped cloud. The probe laser is tuned near resonance and imaged onto a CCD camera with a high resolution lens system. The 2-dimensional velocity distribution should show a strong bimodal character as one achieves BEC. The condensate atoms form a sharp low velocity peak on top of a broad pedestal of thermal atoms.

Several groups around the world have achieved BEC and are intensely studying this new phase of matter. Experiments have been performed which show that the condensate has a well-defined phase and can be interfered with another condensate. Experiments studying the dynamics of condensate formation show that atoms fall into the condensate phase by a process of stimulated scattering (Bosonic stimulation). In other experiments, a fraction of the condensed atoms has been coupled out of the trap in a coherent manner to make an atomic analogue of a pulsed laser. Collective excitations and other dynamics of BECs have also been studied.

While much of the preliminary work with Bose condensates has already been done, there are a lot of interesting experiments waiting to be performed. Bose condensates are becoming the test bed for understanding many phenomena in condensed matter physics since the systems are simple and optical interactions are a powerful diagnostic tool for probing the system *in situ*. The following is a partial list of future experiments: study of two-component Bose systems; simultaneous trapping of bosons and fermions and use of sympathetic cooling to get a degenerate Fermi gas; generation and study of vortices in condensates; coherent quantum tunneling between two condensates (Josephson effect); electromagnetically induced transparency in BEC; nonlinear optical effects and high order susceptibilities. Since this is a young field, only our imagination limits us in the kinds of new experiments that can be performed.

Search for a permanent electric dipole moment

It has long been realized that an atom in its ground state cannot have a permanent electric dipole moment (EDM) unless both parity (P) and time-reversal (T) symmetry are violated[10]. This follows from the Wigner–Eckart theorem, which states that the expectation value of any

vector operator is proportional to the expectation value of the angular momentum operator. The electric dipole moment is a polar vector and changes sign under parity while the angular momentum is an axial vector and does not change sign. Therefore, if the atomic Hamiltonian conserves parity, the expectation value of the dipole moment is uniquely 0. A similar argument holds for time reversal operation, where the angular momentum changes sign but the electric dipole moment does not. Since it is known that the weak interaction violates parity, the existence of a permanent atomic EDM would be a direct indication that time reversal symmetry is violated. The search for an atomic EDM is important because the observed CP violation in neutral kaon decay, which is equivalent to T violation, is rather poorly understood. Several theories put forth to explain kaon decay also predict atomic EDMs, and can be verified or ruled out by EDM searchers.

An experiment to measure atomic EDM can potentially be made much more sensitive by using a laser-cooled cloud of atoms. One way to search for an EDM is to spin polarize a cloud of atoms and look for a precession of the spin in the presence of a strong electric field applied perpendicular to the spin direction. If the atoms had an EDM (which would point along the spin direction from the Wigner–Eckart theorem), the $\mu \times E$ torque would cause the dipoles to precess, analogous to the Larmor precession of spins in an applied magnetic field. By using a laser-cooled atomic cloud instead of a thermal vapour, the signal can be enhanced because the density of atoms in the sample region will be larger. Similarly, the precession rate can be increased because the smaller atom cloud will allow the use of larger electric fields. Both of these enhancements will increase the sensitivity of the experiment. In addition, residual electric field inhomogeneities, which are a potential source of systematic error, can be reduced by using a well localized cold cloud.

Neutral Yb is a good candidate for a laser-cooled EDM experiment[11]. It has a strong transition from $^1S_0 \rightarrow {}^1P_1$ at 398 nm with a relatively short excited state lifetime of 5.5 ns which can be used for efficient laser cooling. Since the ground $^1S_0$ state has no hyperfine structure, there is no need for a repumping beam as in the case of alkali atoms. The odd isotopes ^{171}Yb and ^{173}Yb have non-zero nuclear spins and can be spin polarized for the EDM measurement.

The 398 nm light needed for laser cooling of Yb can be generated by using a nonlinear crystal to double the frequency of a diode laser operating at 796 nm. Since the doubling process is a nonlinear process, its efficiency increases with the light intensity. The power output of commercial single mode cw diode lasers at 796 nm is limited to about 200 mW. Therefore, it is advantageous to use an external power build-up cavity to increase the power available for doubling. One simple

design[12] is to use a bow-tie ring cavity with 4 mirrors, two concave and two plane, as shown in Figure 4. The propagation of a Gaussian beam through the ring cavity can be analysed using the technique of *ABCD* matrices[13] as outlined in Appendix I.

In the design shown in Figure 4, the curved mirrors have a radius of curvature of 18 mm and a separation of 22 mm. The geometrical path length between the curved mirrors via the plane mirrors is 140 mm. The nonlinear element is a 6 mm long $KNbO_3$ crystal. The analysis of Appendix I shows that there are two beam waists in the cavity, a small focus ($w_0 = 12\ \mu m$) between the curved mirrors and a relatively collimated beam ($w_0 = 0.17$ mm) between the plane mirrors. The diode laser output is coupled (with a Faraday isolator to prevent reflections from destabilizing the laser) to the larger beam waist through one of the plane mirrors. The nonlinear crystal is located in the smaller waist where the intensity is higher resulting in higher conversion efficiency. The frequency doubled light is coupled out through one of the curved mirrors. With a cavity Q of 30, the overall conversion efficiency can be as high as 5–10%. The cavity is actively stabilized to be resonant with the frequency of the diode laser by mounting one of the plane mirrors on a peizoelectric transducer and using a servolock loop.

The starting point of the EDM experiment is again a MOT. The MOT is continuously loaded from a Yb oven using what is called a Zeeman slower. The thermal beam emanating from the oven is slowed by a counter-propagating laser beam tuned near resonance for atoms travelling at the mean velocity characteristic of the oven temperature. However, as the atoms absorb light and
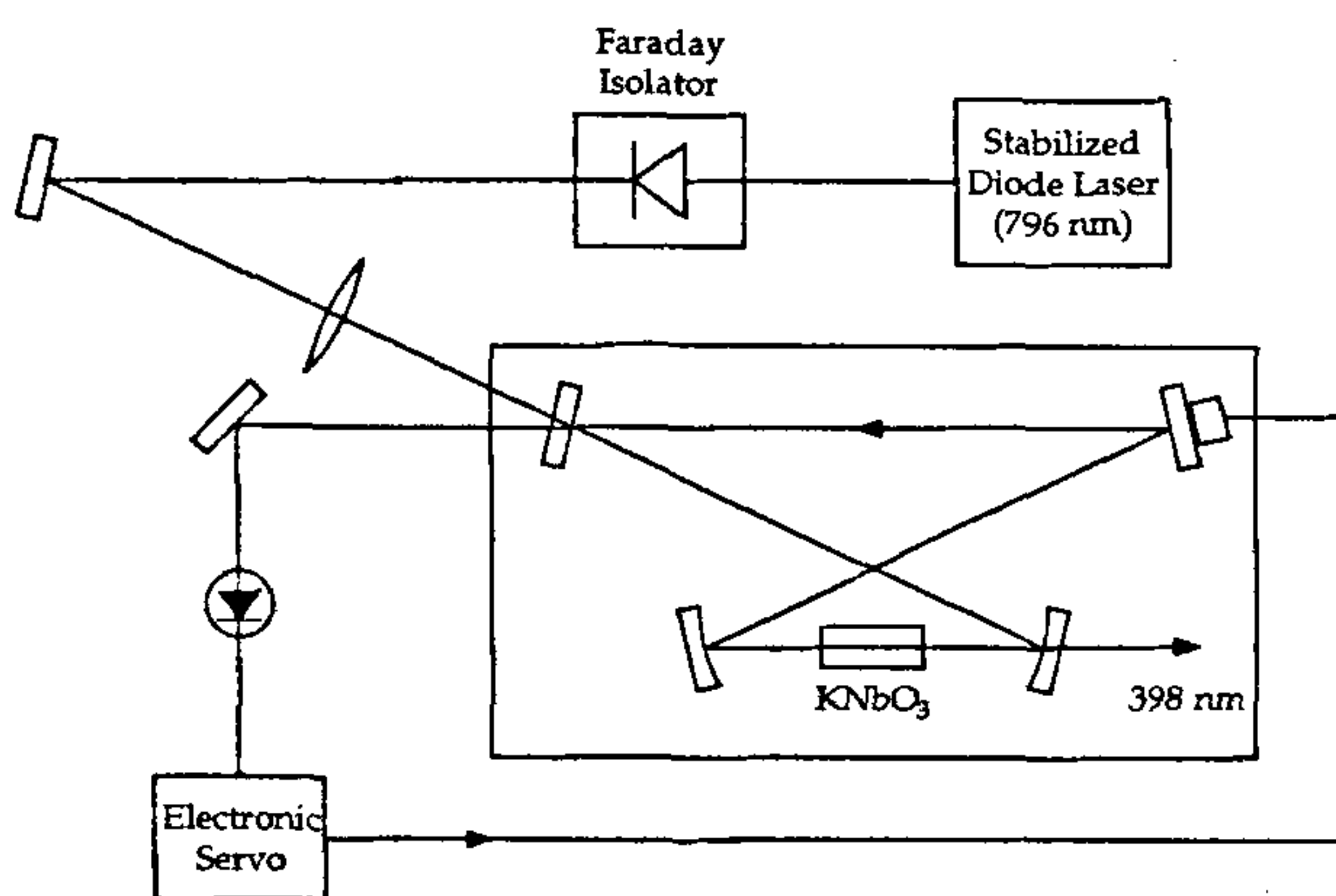

Figure 5. Magnetic field profile for a Zeeman slower for Yb atoms. The atoms emanate from an oven at 300°C. The slowing beam has left circular polarization and drives the $^1S_0$ ($F = 1/2$, $m_F = -1/2$) → $^1P_1$ ($F' = 3/2$, $m_F = -3/2$) transition at 398 nm with an intensity of 58 mW/cm^2. The magnetic field is designed to keep the atoms in resonance with the laser beam as they slow down.

slow down, they soon shift out of resonance. To compensate for the changing Doppler shift, a tapered magnetic field is used. The change in the Zeeman shift of the atomic energy levels is designed to keep the laser near resonance throughout the beam path. For Yb atoms emanating at 300°C, the magnetic field profile for a Zeeman slower is shown in Figure 5. The slowing beam is left circularly polarized and drives the transition from $^1S_0$ ($F = 1/2$, $m_F = -1/2$) → $^1P_1$ ($F' = 3/2$, $m_F = -3/2$). It has an intensity of 58 mW/cm^2 which is the saturation intensity for this transition. As can be seen from the figure, the maximum field required is about 2.8 kG. The short lifetime of 5.5 ns in the excited state means that the atoms cycle photons rapidly and can be stopped over a short distance of about 20 cm. It is possible to deflect the beam away from the slowing beam into the MOT using one-dimensional molasses at an angle of about 30° to the slowing beam[14].

In the EDM experiment, the atoms are spin polarized along, say, the x-axis, an electric field is applied along the z-axis, and the spin precession is measured by measuring the spin component along the y-axis. The y-component of the spin can be obtained by measuring the resonant absorption or off-resonant refraction of a weak probe beam. In the first case, the probe beam is tuned to the atomic transition. The probe is circularly polarized and propagates along the y-direction through the sample. Its absorption depends on the degree of y-polarization of

Figure 4. Schematic for a diode laser frequency doubler. The power output of the diode laser is built up in an external cavity which is of a bow-tie ring cavity design, adapted from ref. 12. The diode laser is isolated from the cavity using a Faraday isolator. Its output is mode matched into the cavity through one of the plane mirrors. The doubling element is a 6 mm long $KNbO_3$ crystal. The frequency doubled light is coupled out through one of the concave mirrors. The cavity length is servo-locked to the frequency of the diode laser using a peizoelectric positioner.
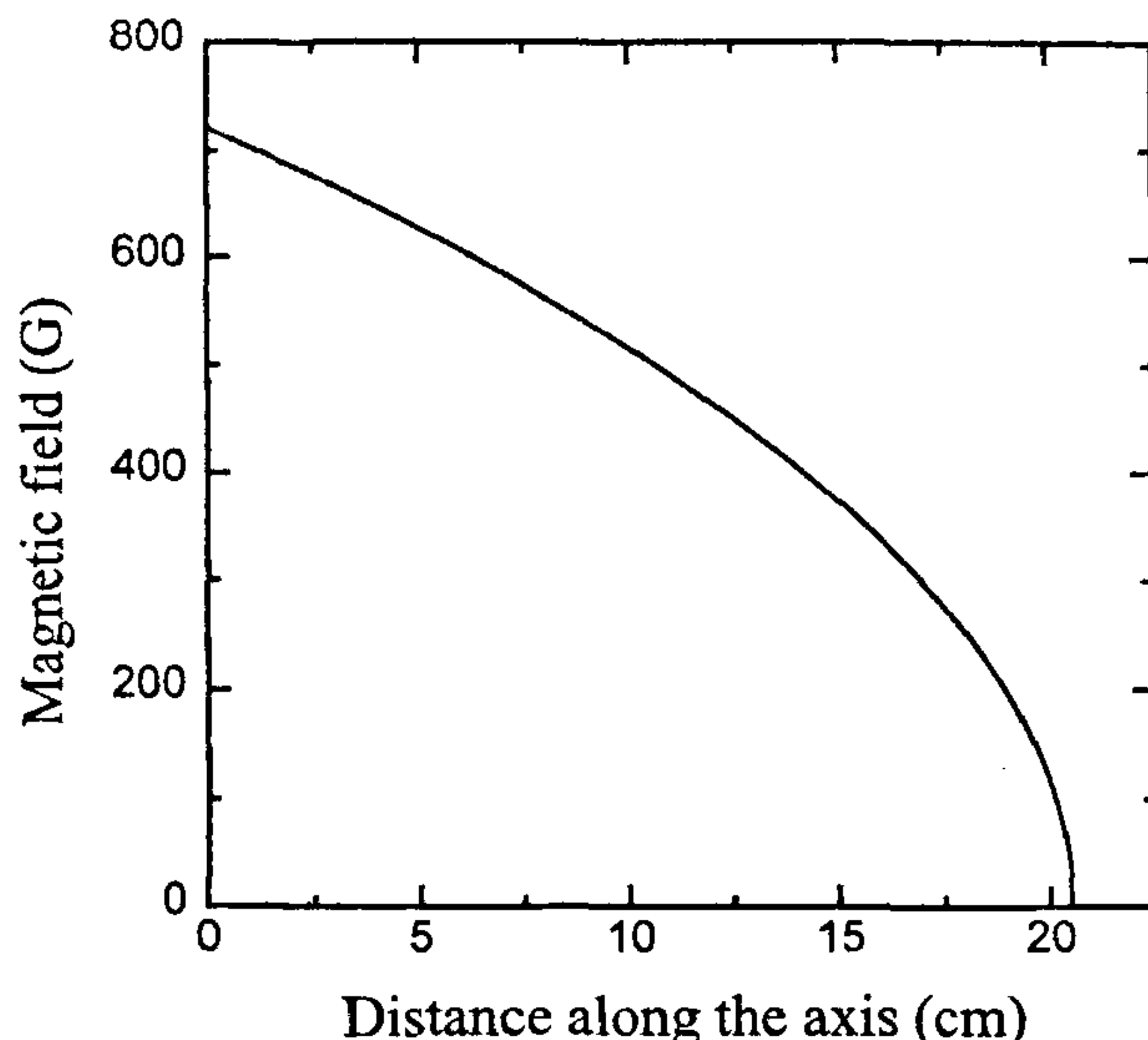
the atoms. It is advantageous to modulate the helicity of the probe and do a lock-in detection so that optical pumping effects average to zero over a cycle[15]. Alternatively, off-resonant light can be used for measuring the y-component of spin. In this case, the probe beam is linearly polarized. The refractive indices for opposite circular polarizations are different depending on the y-polarization of the sample. Since linear polarization can be considered as a superposition of opposite circular polarizations, the plane of polarization gets rotated as the beam traverses the sample, by an amount proportional to the y-polarization of the atoms.

Conclusions

The wide variety of experiments being performed with laser-cooled atoms is constantly expanding. First of all, the quest for ever lower temperatures has resulted in clever cooling schemes which overcome the single photon recoil limit and seem to be limited only by the coherent interaction time in reaching lower temperatures. Cold atoms have been trapped in optical lattices created by intersecting light fields and their dynamics have been studied. Laser-cooled atoms have been used for a novel form of lithography where atoms are directly deposited onto substrates with nanoscale precision. A whole new field of studying collisions between ultra-cold atoms and the formation of weak bound states has been started.

Many of these studies are discussed by last year's Nobel laureates in their Nobel lectures published recently[16-18]. The references contained therein are a good starting point to learn more about the exciting possibilities that laser cooling has opened up. We have only touched on a couple of experiments in this paper. But it is already clear that the advantages of laser-cooled atoms will impact both our fundamental understanding of natural laws and the technology of the future.

Appendix I. Ray tracing through ring cavity

During the passage of a Gaussian beam through an optical system, the parameters $w(x)$ (beam radius) and $R(x)$ (wavefront radius of curvature) transform via a complex bilinear transformation of the form

$$q_{out} = \frac{q_{in}A + B}{q_{in}C + D}, \tag{1}$$

where q is a complex composite of w and R:

$$\frac{1}{q(x)} = \frac{1}{R(x)} - \frac{i\lambda}{\pi w(x)^2} \tag{2}$$

and A, B, C and D are components of the $ABCD$ matrices that are used for geometric ray tracing. From eq. (2), we see that at the location of a beam waist ($R = \infty$ and $w = w_0$), q is pure imaginary and equals x_R, the Rayleigh parameter, given by $(\pi w^2_0/\lambda)$.

The form of the $ABCD$ matrices for ray propagation through various optical elements are:

(a) Propagation through free space by a distance d:

$$\begin{pmatrix} 1 & d \\ 0 & 1 \end{pmatrix}$$

(b) Propagation through a medium of refractive index n by a distance d:

$$\begin{pmatrix} 1 & d/n \\ 0 & 1 \end{pmatrix}$$

(c) Reflection at a mirror of radius of curvature R:

$$\begin{pmatrix} 1 & 0 \\ -2/R & 1 \end{pmatrix}$$

Using these matrices and eqs (1) and (2), we can trace a Gaussian beam through the ring cavity of Figure 4. With values of $R = 18$ mm for the curved mirrors, $R = \infty$ for the plane mirrors, $d = 6$ mm and $n = 2.28$ for the KNbO$_3$ crystal, distance between the curved mirrors = 22 mm, and total geometrical path length between the curved mirrors via the plane mirrors = 140 mm, we find a tight focus with $w_0 = 12$ μm inside the crystal and a relatively collimated beam with $w_0 = 0.17$ mm between the plane mirrors.

In writing the $ABCD$ matrix for case (c), we have assumed normal incidence at the mirror surface. For an arbitrary angle of incidence, the beam propagation in the sagittal plane (plane of incidence) and tangential plane (perpendicular to the plane of incidence) are different. If the angle of incidence at a curved mirror is θ, the $ABCD$ matrix for case (c) is changed by substituting R with $R/\cos\theta$ for the sagittal plane and $R\cos\theta$ for the tangential plane.

1. Macadam, K. B., Steinbach, A. and Wieman, C., *Am. J. Phys.*, 1992, **60**, 1098–1111.
2. Anderson, M. H., *Science*, 1995, **269**, 198–201.
3. Davis, K. B. *et al.*, *Phys. Rev. Lett.*, 1995, **75**, 3969–3973.
4. Weiss, D., *et al.*, in *Light Induced Kinetic Effects on Atoms, Ions and Molecules* (eds Moi, L. *et al.*), ETS Editrice, Pisa, 1991, pp. 35–44.
5. Pritchard, D. E., *Phys. Rev. Lett.*, 1983, **51**, 1336–1339.
6. Bergeman, T., Erez, G. and Metcalf, H. J., *Phys. Rev.*, 1987, **A35**, 1535–1545.
7. Pritchard, D. E., Helmerson, K. and Martin, A. G., in Proceedings of the 11th International Conference on Atomic Physics (eds Haroche, S., Gay, J. C. and Grynberg, G.), World Scientific, Singapore, 1989, pp. 179–181.
8. Ketterle, W. *et al.*, *Phys. Rev. Lett.*, 1993, **70**, 2253–2256.
9. Davis, K. B. *et al.*, *Phys. Rev. Lett.*, 1995, **74**, 5202–5205.
10. Commins, E. D., *Phys. Scri.*, 1993, **T46**, 92–100.
11. Das, B. P., private communication, 1997.
12. Zimmermann, C., Hemmerich, A. and Hänsch, T. W., in *Advances in Solid State Physics, Festkörperprobleme 34* (ed. Helbig, R.), Vieweg, Braunschweig, 1994, pp. 51–63.
13. Kogelnik, H. and Li, T., *Appl. Opt.*, 1966, **5**, 1550–1567.
14. Witte, A., Kisters, Th., Riehle, F. and Helmcke, J., *J. Opt. Soc. Am.*, 1992, **B9**, 1030–1037.
15. Murthy, S. A., Krause, D., Jr., Li, L. and Hunter, L. R., *Phys. Rev. Lett.*, 1989, **63**, 965–968.
16. Chu, S., *Rev. Mod. Phys.*, 1998, **70**, 685–705.
17. Cohen-Tannoudji, C. N., *Rev. Mod. Phys.*, 1998, **70**, 707–719.
18. Phillips, W. D., *Rev. Mod. Phys.*, 1998, **70**, 721–741.